UCRL-17322

University of California

Ernest O. Lawrence Radiation Laboratory

ON-LINE α SPECTROSCOPY OF NEUTRON-DEFICIENT RADIUM ISOTOPES

TWO-WEEK LOAN COPY

This is a Library Circulating Copy
which may be borrowed for two weeks.
For a personal retention copy, call
Tech. Info. Division, Ext. 5545

Berkeley, California

DISCLAIMER

This document was prepared as an account of work sponsored by the United States Government. While this document is believed to contain correct information, neither the United States Government nor any agency thereof, nor the Regents of the University of California, nor any of their employees, makes any warranty, express or implied, or assumes any legal responsibility for the accuracy, completeness, or usefulness of any information, apparatus, product, or process disclosed, or represents that its use would not infringe privately owned rights. Reference herein to any specific commercial product, process, or service by its trade name, trademark, manufacturer, or otherwise, does not necessarily constitute or imply its endorsement, recommendation, or favoring by the United States Government or any agency thereof, or the Regents of the University of California. The views and opinions of authors expressed herein do not necessarily state or reflect those of the United States Government or any agency thereof or the Regents of the University of California.

To be Submitted to Phys. Rev.
Section 55.2

UCRL-17322
Preprint

UNIVERSITY OF CALIFORNIA

Lawrence Radiation Laboratory
Berkeley, California

AEC Contract No. W-7405-eng-48

ON-LINE α SPECTROSCOPY OF NEUTRON-DEFICIENT RADIUM ISOTOPES

Kalevi Valli, William Treytl, and Earl K. Hyde

February 1967

ON-LINE α SPECTROSCOPY OF NEUTRON-DEFICIENT RADIUM ISOTOPES*

Kalevi Valli, William Treytl, and Earl K. Hyde

Lawrence Radiation Laboratory
University of California
Berkeley, California

February 1967

ABSTRACT

Isotopes of radium lighter than mass 215 were studied at the Heavy Ion Linear Accelerator by bombardment of ^{206}Pb with ^{12}C and ^{197}Au with ^{19}F. Silicon (Au) surface-barrier detectors were used in on-line measurements to measure α-decay characteristics. Mass number assignments of ^{214}Ra through ^{206}Ra were made on the basis of excitation functions and genetic relationships with francium, emanation, and astatine isotopes. Half-lives and accurate α energies were determined for the radium isotopes, and the α energy of ^{214}Fr was corrected. Alpha and β branchings were measured for ^{213}Ra and ^{214}Ra. Some systematic trends in the alpha decay energies were interpreted in terms of a weakening of neutron and proton pairing energies near closed shells.

I. INTRODUCTION

We are engaged in an extensive study of the α-decay properties of the neutron-deficient isotopes of elements between lead and thorium. Many nuclides in this region are known from previous reports[1] but improved performance of the Berkeley Heavy Ion Linear Accelerator (HILAC) and further developments in on-line techniques have made it possible to collect more accurate information and to detect previously unknown activities. The information so obtained is interesting in its own right and is valuable in connection with the method of closed α-β decay cycles for improving and extending estimates of atomic masses, α- and β-decay energies, and neutron-and proton-binding energies. In addition, in experiments designed to investigate transuranium nuclides, α-active nuclides in the lead to thorium region may appear either as the result of rapid and complex decay chains or, more usually, through the influence of trace impurities on the target materials. Hence it is desirable to have as complete a knowledge of these nuclides as is possible.

In three previous papers we have reported α-decay properties of light isotopes of polonium and astatine,[2] radon,[3] and francium.[4] In this report light radium isotopes are considered.

Griffioen and Macfarlane[5] have obtained α energies and half-lives for ^{212}Ra, ^{213}Ra, and ^{214}Ra. From the systematic trends of α decay in this region several more radium isotopes can be expected to have half-lives long enough to be detected with the present method. In this work we observed a number of new activities which, on the basis of half-lives, accurate α energies, and excitation functions, can be attributed to ^{206}Ra through ^{214}Ra. Excitation functions of the daughter activities were also determined. Careful inspection of the data provided multiple verification of most of the radium mass number assignments.

II. EXPERIMENTAL

Our experimental technique was a modification of the method used by Macfarlane and Griffioen.[6] Essentially, the products recoiling from a thin target were slowed to thermal energies in a helium atmosphere and swept through a small nozzle onto a catcher foil in an adjacent vacuum chamber. The products thus deposited were then quickly positioned in front of a Si (Au) surface-barrier detector. Small amounts of activity were collected on the catcher foil in less than 50 msec while the collection time for the major part was of the order of seconds. In a typical experiment recoil activity was alternatively collected for a fraction of a second and counted for the same period, with the cycle repeated over a period of 10 to 20 minutes. The apparatus, the electronics, and the special energy calibration method are described in a previous article.[2]

The reactions used in the study were:

$$^{197}Au(^{19}F,xn)^{216-x}Ra \quad \text{and}$$

$$^{206}Pb(^{12}C,xn)^{218-x}Ra \quad ,$$

where x refers to the number of evaporated neutrons. The targets were 2.5 mg/cm^2 gold leaf and separated ^{206}Pb (97.22% ^{206}Pb, 1.34% ^{207}Pb, 1.39% ^{208}Pb, according to the supplier, Oak Ridge National Laboratory) electroplated on 2.3 mg/cm^2 nickel foil. The thickness of the ^{206}Pb target was about 0.3 mg/cm^2.

Maximum beam energy was 197 MeV for ^{19}F and 125 MeV for ^{12}C. Lower energy beams were obtained by inserting stacks of 1.72 mg/cm^2

aluminum absorber foils in front of the target.[2] The range-energy relationships of Northcliffe[7] were used to calculate the energy degradation in the absorbers.

The excitation functions were measured starting at the Coulomb barrier and progressively increasing the beam energy until the maximum energy was reached, or vice versa, starting at full beam energy and ending at the barrier. The total integrated beam current was the same for all runs, each of which required about 15 minutes, with an interval of about three minutes between measurements. With this time schedule, some distortion of the excitation functions of the longer lived daughter activities was observed owing to the recording of residual activity from one measuring period to the next.

In separate experiments half-lives of individual α peaks were determined with the techniques outlined previously.[2]

III. RESULTS

A number of representative α spectra obtained at different bombarding energies are shown in Figs. 1 and 2. Excitation functions derived from the complete sets of α spectra are presented in Figs. 3 and 4. The first of these shows the yield versus bombarding energy curves for individual radium and daughter activities from the reactions $^{206}Pb(^{12}C,xn)^{218-x}Ra$, while Fig. 4 displays the corresponding information for the $^{197}Au(^{19}F,xn)^{216-x}Ra$ reactions. The radium yield curves have the regular behavior expected of compound nucleus reactions so that tentative mass number assignments can be made to the unknown radium activities. These assignments are bolstered by the similarity in shape of the yield curves for francium daughters (produced by electron capture of the radium parents) and emanation daughters (produced by α decay of radium parents). In several cases even the astatine granddaughter was observed. The daughters in turn were identified on the basis of their α-particle energies and half-lives. The behavior of the radon daughter activity was particularly reliable since any radon produced by direct reactions would fail to collect; the observed radon activity must have been formed by the decay of radium on the catcher foil.

In the case of the radium isotopes with half-lives 3.8 sec or less (mass number below 211) the observed radium intensities are much less than the observed intensities for the daughters. This is a result of decay in flight of the short-lived radium parent before it can be swept from the chamber and collected on the catcher foil. When this occurs the longer-lived francium daughter or astatine granddaughter activity is collected and counted. This effect does not prevent

the observation and identification of the radium isotope but it interferes with the determination of α/EC branch ratios and with the estimation of reaction cross sections for production of the shorter-lived isotopes.

Details of the analysis of the excitation curves are given in the following paragraphs where the individual radium isotopes are discussed. To aid the discussion some of the excitation function data have been replotted in Fig. 5 in a manner to classify the relation of parent and daughter activities. A summary of the new radium results is given in Table I. The quoted errors are conservative limits covering the total spread of many individual measurements and are substantially greater than the statistical uncertainty.

A. Radium-214

Griffioen and Macfarlane[5] have reported an α energy of 7.17 MeV and a half-life of 2.6 sec for ^{214}Ra. The corresponding values obtained in the present investigation are 7.136 MeV and 2.6±0.2 sec. The peak is shown in Fig. 1. The assignment is based on the excitation function of the peak shown in Fig. 3. Additional evidence is provided by the excitation function of the composite 6.037-MeV peak which belongs to ^{209}Rn and to ^{210}Rn, the latter being the α-decay daughter of ^{214}Ra.

An α energy of 8.55 MeV and a half-life of 3.9 msec have been reported for ^{214}Fr.[5] The weak peak at 8.430 MeV in the spectra obtained from the ^{206}Pb + ^{12}C reactions (Fig. 1) must be the same activity in equilibrium with its ^{214}Ra parent. Its apparent half-life is 2.6 sec, equal to that of ^{214}Ra, and its

excitation function in Fig. 3 follows that of ^{214}Ra. From the intensity ratio of the peak at 8.430 MeV to that at 7.136 MeV the electron-capture branching of ^{214}Ra was determined to be 0.09±0.03%.

B. Radium-213

The α spectrum of ^{213}Ra is shown in Fig. 1. The energies and relative intensities of the three observed peaks are: 6.730 MeV, 45±2%; 6.623 MeV, 49±2%; and 6.520 MeV, 6±1%. The half-life was measured to be 2.75±0.15 minutes. Values reported previously were: α energies 6.74 and 6.61 MeV, and half-life 2.7 minutes.[5]

The excitation functions in Fig. 3 show clearly that the three peaks belong to one isotope. The yield maxima occur at the bombarding energy expected for the ^{206}Pb(^{12}C,5n)^{213}Ra reaction. Furthermore the yield curve of the electron-capture daughter, ^{213}Fr, has the same shape at low beam energies, although at higher energies most of the ^{213}Fr is probably produced by direct reactions. The composite ^{209,210}Rn excitation curve also agrees with this assignment. The weak α peak at 8.090 MeV belongs to ^{213}Rn, the electron-capture daughter of ^{213}Fr.[4] Its excitation function is shown in Fig. 3.

The α and electron-capture branches of ^{213}Fr are known to be 99.4 and 0.57%, respectively.[4] Thus, the α and electron-capture branches of ^{213}Ra can be determined from the present spectra. Under the assumption that direct production of ^{213}Fr is negligible at ^{12}C-beam energies lower than 85 MeV, the α branch of ^{213}Ra is 80±5% and the electron-capture branch 20±5%.

In a few spectra taken close to 85-MeV beam energy (Fig. 1) where the contributions of ^{212}Fr groups are small, a weak peak can be seen at 6.408±005 MeV. It is reasonable to assign it to ^{213}Ra. Unfortunately, no reliable half-life was obtained for this peak, and its excitation function (Fig. 3) cannot be determined separately from that of the interfering ^{212}Fr groups. If the assignment to ^{213}Ra is correct, the relative intensity of the peak is 0.4±0.2%.

C. Radium-212 and Radium-211

Systematic trends in α decay indicate that α energies of ^{212}Ra and ^{211}Ra should be nearly the same. An α peak at 6.90 MeV (Figs. 1 and 2) has a broad excitation function (Figs. 3 and 4), which is most logically explained as a composite curve for these two isotopes. Moreover, the composite excitation curve for the ^{208,207}Em daughter pair (Fig. 5(a)) is similar to the composite parent curve. The excitation function of ^{211}Fr (Fig. 5(a)), the electron-capture daughter of ^{211}Ra, is combined with that of ^{210}Fr because of the similarity in α-particle energies, but the low energy part of the composite curve is chiefly ^{211}Fr and it provides good evidence for the position of ^{211}Ra in the composite ^{211,212}Ra parent curve. The intensity of ^{212}Fr α activity was too low to permit construction of good excitation functions because the electron-capture branching of ^{212}Ra is low, the half-life of ^{212}Fr is long (19.3 min), and its α decay is complex.

In careful measurements made at beam energies where ^{212}Ra was predominant over ^{211}Ra we determined an α energy of 6.896 MeV and a half-life of 13±2 sec. At beam energies where ^{211}Ra was the principal activity we determined values of

6.910 MeV and 15±2 sec. The values reported previously for ^{212}Ra are 6.90 MeV and 18 sec[5]; no reports exist for ^{211}Ra.

D. Radium-210 and Radium-209

From the systematic trends in properties, the α energies of ^{210}Ra and ^{209}Ra are also expected to be very similar. A peak is seen at 7.01 MeV (Figs. 1 and 2) which we may attribute to these isotopes. The excitation function of this peak (Fig. 5(b)) is broad and is similar to the composite yield curve of the α daughters, ^{206}Rn and ^{205}Rn (Fig. 5(b)). The excitation functions of the β-decay daughters, ^{210}Fr and ^{209}Fr are combined with those of ^{211}Fr and ^{208}Fr, respectively. Their behavior is in agreement with the radium assignments. The yield curve of the granddaughter, ^{205}At, is also in agreement after allowance is made for its shift toward higher-beam energies caused by the 26-min half-life; i.e., by the persistence of some ^{205}At α activity from one measuring period to the next.

From measurements made at a 105 MeV ^{19}F beam energy where ^{210}Ra predominates over ^{209}Ra we measured an α energy of 7.018 MeV and a half-life of 3.8±0.2 sec. Properties of ^{209}Ra were measured on samples prepared at a beam energy of 140 MeV. The α energy and half-life are 7.008 MeV and 4.7±0.2 sec, respectively.

E. Radium-208 and Radium-207

Another pair of radium isotopes with similar α energies is ^{208}Ra and ^{207}Ra. Alpha-energy calibrations were made at several beam energies to determine whether the peak at 7.131 MeV in Fig. 2 consists of two unresolved components. Only one value was observed, however, and it was attributed both to ^{208}Ra and ^{207}Ra. The half-life of the group was also determined at several beam energies. Values between 1.1 and 1.4 sec were observed, the shorter ones coming systematically from measurements at lower beam energies. Therefore, 1.3±0.2 sec is reported for ^{207}Ra and 1.2±0.2 sec for ^{208}Ra. Since these half-life errors overlap, the burden of proof for the existence of two isotopes falls on the observation of the daughter products.

The excitation function of the 7.131-MeV peak in Fig. 5(c) is broad which indicates that it belongs to two isotopes. If small deviations caused by experimental difficulties are ignored, the yield maxima of ^{207}Fr and ^{203}At in Fig. 5(c) fall at the same beam energy as the estimated excitation maximum of ^{207}Ra. Similarly, the yield maxima of ^{208}Fr and ^{204}At fall at the beam energy expected for the maximum yield of ^{208}Ra.

F. Radium-206

The weak α group at 7.270 MeV in Fig. 2 belongs to ^{206}Ra. Its half-life was measured to be 0.4±0.2 sec. The excitation function of this peak resembles those of ^{206}Fr, ^{202}At, and ^{202m}At in Fig. 5(d). Francium-206 is the electron capture daughter of ^{206}Ra; ^{202}At and ^{202m}At are granddaughters.

Radium isotopes lighter than ^{206}Ra can be expected to have half-lives too short to be detected with the present equipment. The relatively strong ^{205}Fr group at 6.917 MeV and ^{201}At group at 6.342 MeV in Fig. 2 (see also Fig. 5 (d)) indicate that ^{205}Ra was produced but that it decayed to ^{205}Fr and ^{201}At before the recoil atoms were collected.

G. Polonium Isotopes

In the bombardment of gold with 172 MeV fluorine ions α activity of polonium appeared in the spectra (Fig. 2). The yield of these isotopes dropped off quickly with decrease in energy of the fluorine ions and do not show any clear relationship to the yields of the radium isotopes. As it is most likely these polonium isotopes were produced by some type of partial transfer reaction, not involving the initial production of radium isotopes, we do not discuss them in this paper.

IV. DISCUSSION

The general features of the radium isotopes are similar to those of the neighboring elements discussed in our previous reports.[2-4] The dependence of α-decay energy on neutron number shown in Fig. 6 demonstrates this quite clearly. There is a sharp discontinuity at 126 neutrons and a regular step-like behavior below 126 neutrons. The decay energies of the even-neutron isotopes are higher and the decay energies of the odd-neutron isotopes lower than the averages corresponding to a smooth variation with mass number. This indicates that the steps are a consequence of the pairing of neutrons, and more specifically that the pairing energy is stronger in the daughter than in the parent. In other words, the neutron-pairing energy decreases as the 126-neutron closed shell is approached. This behavior has been noted by other authors,[12,13] but the new radium isotopes provide additional evidence for the regularity of this feature. We note also that the curves for different elements are not equally spaced. The curve for an odd-proton element is closer to the one of the higher even-proton element; e.g., the francium curve is closer to radium than radon. This suggests that the unequal spacings are a consequence of the pairing of protons and that the proton pairing energy is greater in the parent than in the daughter. Stated another way, the proton-pairing energy increases as more protons are added beyond the 82 closed shell. Thus, the steplike behavior and the unequal spacings of the curves can be explained as a result of a weakening of the neutron- and proton-pairing energies as the closed shell configurations (126 and 82 nucleons) are approached.

A brief inspection of the existing data shows that this trend of weaker pairing near the shell is valid as well on the neutron-rich side of the 126-neutron shell. The step-like behavior is reversed in the sense that the even-neutron isotopes are depressed relative to the odd-neutron isotopes but the spacings between elements remain the same as on the neutron deficient side. The principle seems valid also around other closed shells although it is less pronounced. This behavior provides a useful method for predicting and checking experimental results.

The new data presented in this paper are useful for extending the table of nuclear masses by the general method of α-β decay energy cycles. The masses so obtained are valuable in turn for the derivation of other quantities such as neutron- and proton-separation energies. The most up-to-date published review of α-β decay cycles and masses is that of Viola and Seaborg.[12] In Table II we compare our experimental α Q-values with the experimental and estimated values given by these authors. The results establish the quality of the previous estimates and permit an extension of them to even lighter nuclei.

In this paper we are concerned with the products of the heavy ion induced nuclear reactions rather than the reactions themselves. However, it is easy to extract one quantity of some interest for the excitation function curves. From the beam energy at the maximum yield of each radium isotope, from the Q-value of the reaction, and from the neutron separation energies of the isotopes involved in the evaporation chain, one can deduce the average amount of energy dissipated in neutron kinetic energy plus γ energy in each neutron evaporation step. How this is done is covered in the discussion of a previous paper.[4] It is known

from previous work of Alexander and Simonoff[14] and of Kaplan[15] that in heavy ion reactions involving rare-earth targets 4.8 to 6.3 MeV is dissipated for each neutron evaporated. In our analysis of the Au + F results in Fig. 4 we find that an average of 4.8 MeV is required in the evaporation of the first 4 neutrons and the energy dissipated in the evaporation of the next 6 neutrons varies between 6.0 and 8.1 MeV.

ACKNOWLEDGMENT

We thank Albert Ghiorso for his interest and encouragement in this work. We are indebted to Charles Corum for equipment design and to the HILAC crew for operation of the accelerator.

FOOTNOTE AND REFERENCES

*This work was done under the auspices of the U. S. Atomic Energy Commission.

1. See summary in E. K. Hyde, I. Perlman, and G. T. Seaborg, The Nuclear Properties of Heavy Elements (Prentice Hall, Inc., Englewood Cliffs, New Jersey, 1964) p. 1060-1107.

2. W. Treytl and K. Valli, University of California, Lawrence Radiation Laboratory Report UCRL-17194, October 1966 (submitted for publication in Nucl. Phys., 1967).

3. K. Valli, M. J. Nurmia, and E. K. Hyde, University of California, Lawrence Radiation Laboratory Report UCRL-16735, December 1966 (submitted for publication in Phys. Rev., 1967).

4. K. Valli, E. K. Hyde, and W. Treytl, University of California, Lawrence Radiation Laboratory Report UCRL-17272, 1967.

5. R. D. Griffioen and R. D. Macfarlane, unpublished results cited in Ref. 1, p. 1104.

6. R. D. Macfarlane and R. D. Griffioen, Nucl. Instr. 24, 461 (1963).

7. J. C. Northcliffe, Phys. Rev. 120, 1744 (1960).

8. A. Rytz, Helv. Phys. Acta 34, 240 (1961).

9. G. Bastin-Scoffier, Compt. Rend. 254, 3854 (1962).

10. R. D. Griffioen and R. D. Macfarlane, Phys. Rev. 133, 31373 (1964).

11. W. Treytl, E. K. Hyde, and K. Valli, University of California, Lawrence Radiation Laboratory Report UCRL-17405, 1967 (under preparation).

12. J. O. Rasmussen, "Alpha Decay" in Alpha-β-γ Spectroscopy, K. Siegbahn ed. (1965).

13. V. E. Viola, Jr., and G. T. Seaborg, J. Inorg. Nucl. Chem. 28, 697 (1966).

14. J. M. Alexander and G. N. Simonoff, Phys. Rev. 130, 2383 (1963).

15. M. Kaplan, Phys. Rev. 143, 894 (1966).

Table I. Present results compared with those of Griffioen and Macfarlane (Ref. 5). The following energy standards were used: ^{212}Po 8.7854 MeV, ^{215}Po 7.3841 MeV, ^{219}Em 6.8176 MeV, ^{211}Bi 6.6222 MeV, ^{212}Bi 6.0898 MeV, ^{212}Bi 6.0506 MeV (Ref. 8); ^{216}Po 6.7772 MeV, ^{220}Rn 6.2884 MeV, ^{224}Ra 5.6840 MeV (Ref. 9).

	This work			Griffioen and Macfarlane		
Isotope	Alpha energy MeV	Half-life	%	Alpha energy MeV	Half-life	%
^{214}Ra	7.136±0.005	2.6 ±0.2 sec		7.17	2.6 sec	
^{213}Ra	6.730±0.005	2.75±0.15 min	45±2	6.74	2.7 min	~50
	6.623±0.005	2.75±0.15 min	49±2	6.61	2.7 min	~50
	6.520±0.005	2.75±0.15 min	6±1			
^{212}Ra	6.896±0.005	13 ±2 sec		6.90	18 sec	
^{211}Ra	6.910±0.005	15 ±2 sec				
^{210}Ra	7.018±0.005	3.8 ±0.2 sec				
^{209}Ra	7.008±0.005	4.7 ±0.2 sec				
^{208}Ra	7.131±0.005	1.2 ±0.2 sec				
^{207}Ra	7.131±0.005	1.3 ±0.2 sec				
^{206}Ra	7.270±0.005	0.4 ±0.2 sec				
^{214}Fr	8.430±0.008			8.55	3.9 msec	

Table II. Comparison of α Q-values[a].

Isotope	Experimental (this work)	Experimental or estimated value given by Viola and Seaborg
^{214}Ra	7.272	7.313
^{213}Ra	6.859[b]	6.894
^{212}Ra	7.028	7.039
^{211}Ra	7.044	7.070 est
^{210}Ra	7.154	7.150 est
^{209}Ra	7.144	7.150 est
^{208}Ra	7.271	7.210 est
^{207}Ra	7.272	-
^{206}Ra	7.414	-

[a]The Q-value is the α-particle energy for the ground-state transition corrected for the recoil energy of the daughter nucleus.

[b]In this case the assumption is made that the most energetic α group is a ground-state transition.

Figure Captions

Fig. 1. Alpha spectra showing radium and daughter activities from the reactions $^{206}Pb(^{12}C,xn)^{218-x}Ra$ at three beam energies. Measuring times were 11 min and the beam current was 0.1 μA. Two catcher foils were flipped between alternate collection and measuring positions at a rate of once per sec.

Fig. 2. Alpha spectra showing radium and daughter activities from the reactions $^{197}Au(^{19}F,xn)^{216-x}Ra$ at three beam energies. Measuring time was 1.5 h for the topmost spectrum, 19 min for the two other spectra. Two catcher foils were flipped between alternate collection and measuring positions at a rate of twice per second. Beam current was 0.5 μA.

Fig. 3. Excitation functions of the radium and daughter activities produced in the reactions $^{206}Pb(^{12}C,xn)^{218-x}Ra$. The curves were run from high to low beam energies. Measuring times were 11 min and the intervals between them 3 to 5 min. See the caption of Fig. 1 for other details.

Fig. 4. Excitation functions of the radium and daughter activities produced in the reactions $^{197}Au(^{19}F,xn)^{216-x}Ra$. The curves were run from low to high beam energies. Measuring times were 19 min and the intervals between them 3 to 4 min. See the caption of Fig. 2 for other details.

Fig. 5. Data from Fig. 4 replotted in order to clarify the parent-daughter relationship of certain nuclides.

Fig. 6. Alpha energy versus neutron number for different elements in the area below 126-neutron shell and above 82-proton shell. The solid circles indicate energies assigned to ground-state α decay. The crosses represent α energies assigned to isomeric states. The open circles are α transitions to excited levels at the daughter nuclei (α fine structure). The actinium data come from a study to be reported (Ref. 11).

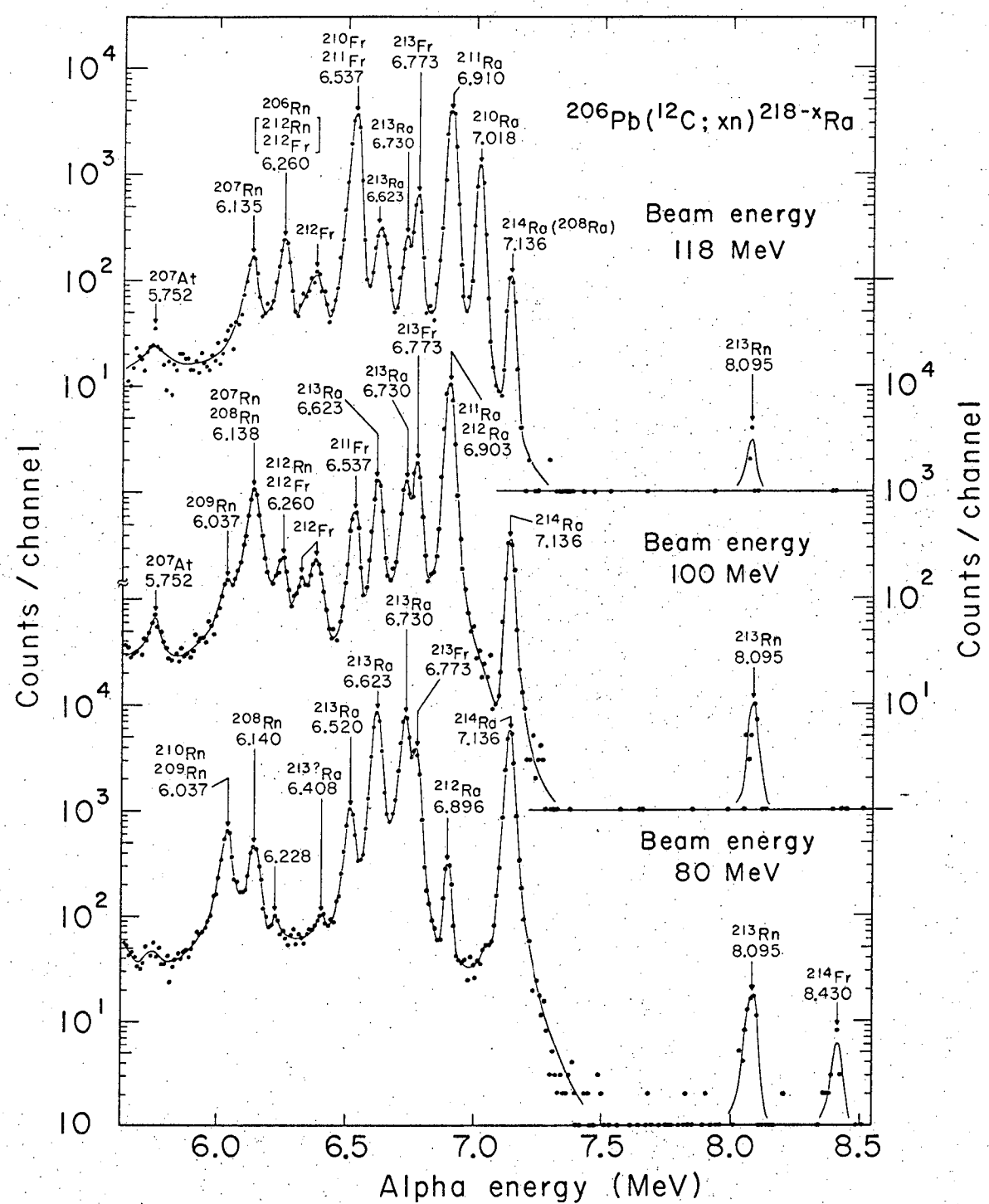
$^{206}Pb(^{12}C; xn)^{218-x}Ra$
Beam energy 118 MeV
Beam energy 100 MeV
Beam energy 80 MeV
Counts / channel
Alpha energy (MeV)
6.0
6.5
7.0
7.5
8.0
8.5
10^4
10^3
10^2
10^1
10
^{207}At 5.752
^{207}Rn 6.135
^{206}Rn [^{212}Rn ^{212}Fr] 6.260
^{212}Fr
^{210}Fr ^{211}Fr 6.537
^{213}Ra 6.623
^{213}Ra 6.730
^{213}Fr 6.773
^{211}Ra 6.910
^{210}Ra 7.018
^{214}Ra (^{208}Ra) 7.136
^{213}Rn 8.095
^{207}Rn ^{208}Rn 6.138
^{209}Rn 6.037
^{212}Rn ^{212}Fr 6.260
^{211}Fr 6.537
^{211}Ra ^{212}Ra 6.903
^{214}Ra 7.136
^{210}Rn ^{209}Rn 6.037
^{208}Rn 6.140
6.228
$^{213?}Ra$ 6.408
^{213}Ra 6.520
^{212}Ra 6.896
^{214}Fr 8.430
XBL671-181A

Fig. 1

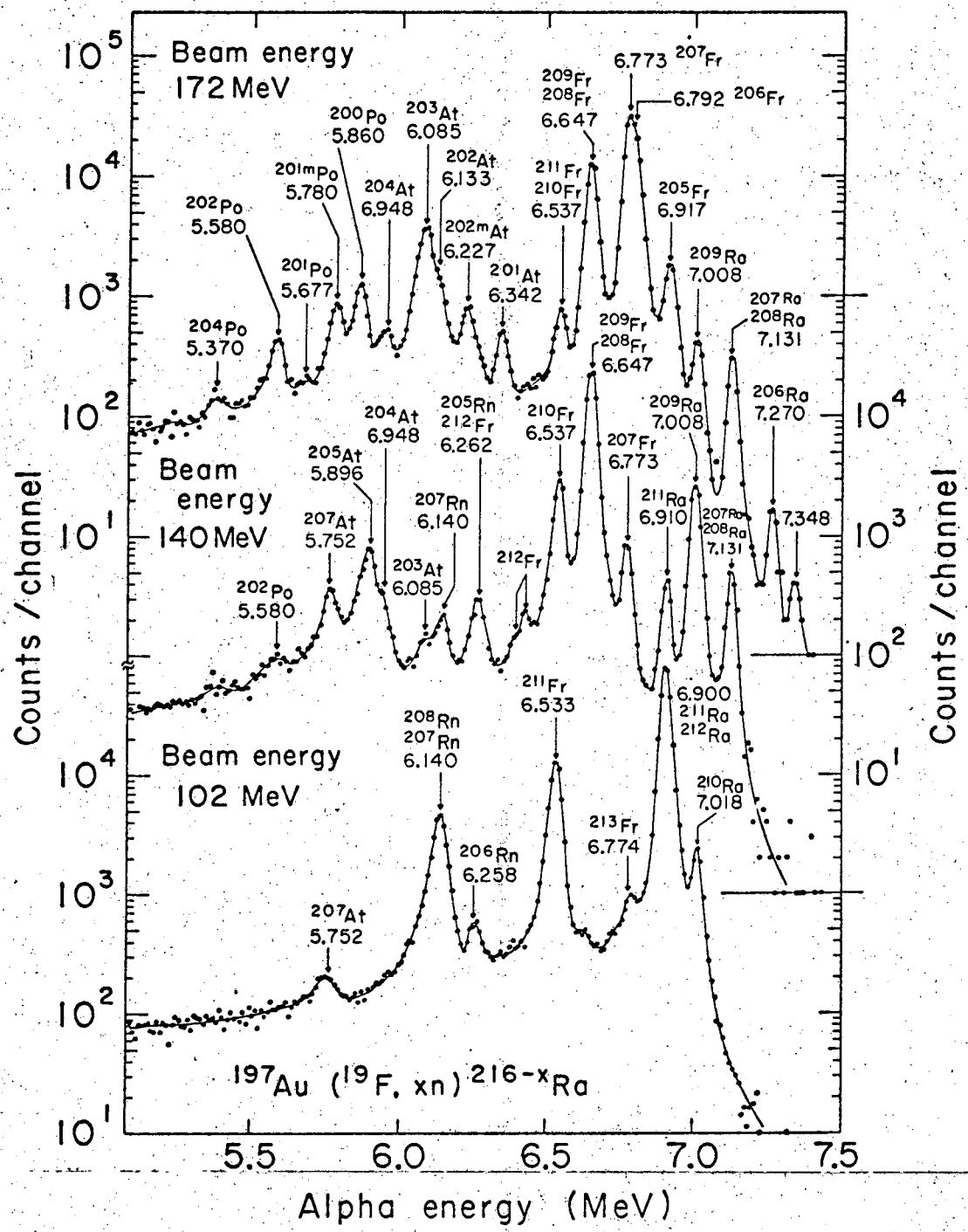
Beam energy
172 MeV
Beam energy
140 MeV
Beam energy
102 MeV
^{197}Au (^{19}F, xn) $^{216-x}$Ra
Counts /channel
Counts /channel
Alpha energy (MeV)
5.5
6.0
6.5
7.0
7.5
10^1
10^2
10^3
10^4
10^5
^{202}Po 5.580
^{204}Po 5.370
^{201m}Po 5.780
^{201}Po 5.677
^{200}Po 5.860
^{204}At 6.948
^{203}At 6.085
^{202}At 6.133
^{202m}At 6.227
^{201}At 6.342
^{209}Fr ^{208}Fr 6.647
^{211}Fr ^{210}Fr 6.537
6.773 ^{207}Fr
6.792 ^{206}Fr
^{205}Fr 6.917
^{209}Ra 7.008
^{207}Ra ^{208}Ra 7.131
^{206}Ra 7.270
^{205}At 5.896
^{207}At 5.752
^{204}At 6.948
^{203}At 6.085
^{207}Rn 6.140
^{205}Rn ^{212}Fr 6.262
^{212}Fr
^{210}Fr 6.537
^{207}Fr 6.773
^{211}Ra 6.910
^{207}Ra ^{208}Ra 7.131
7.348
^{208}Rn ^{207}Rn 6.140
^{211}Fr 6.533
6.900 ^{211}Ra ^{212}Ra
^{210}Ra 7.018
^{213}Fr 6.774
^{206}Rn 6.258
^{207}At 5.752
XBL 671-180A

Fig. 2

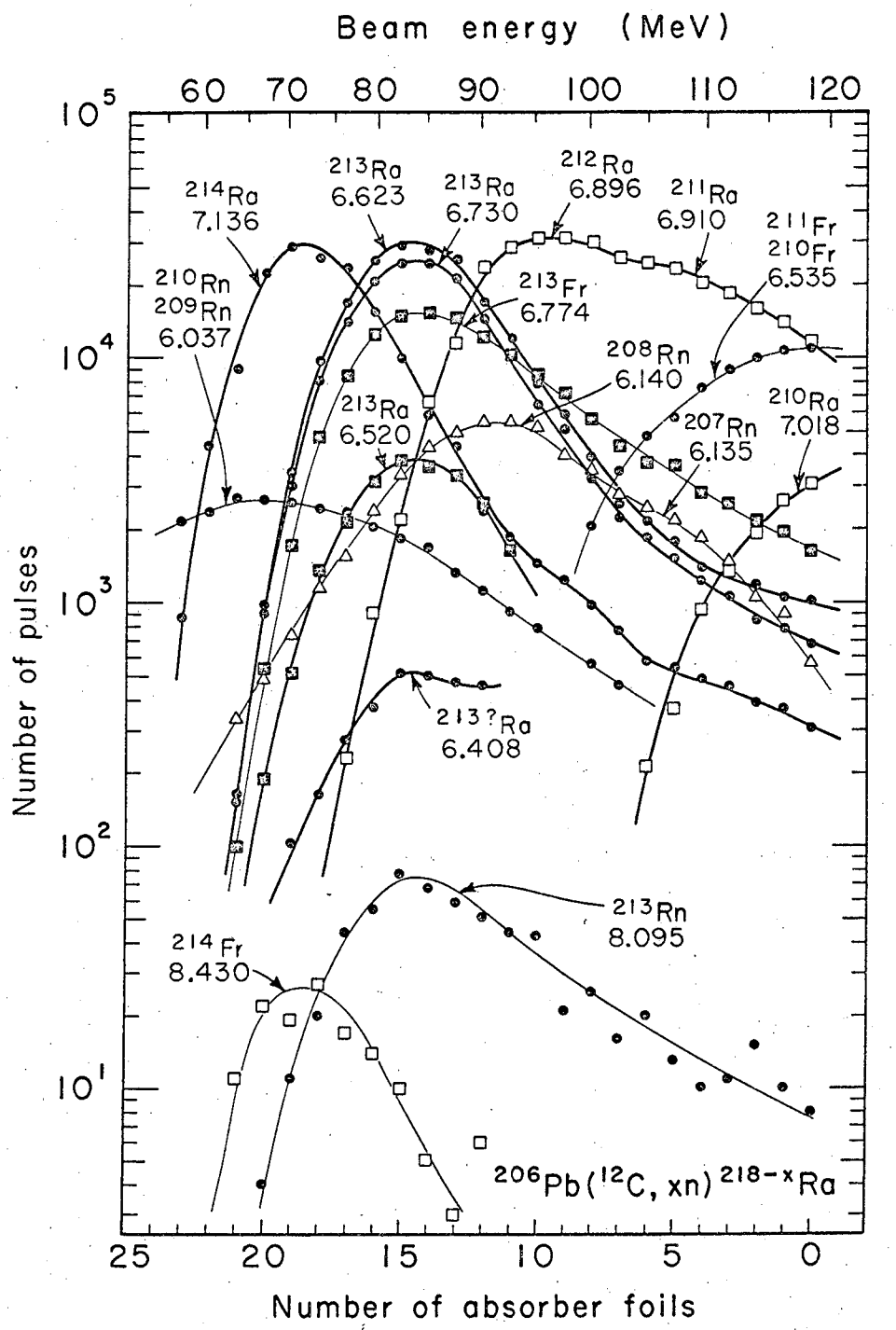

XBL 671-178A

Fig. 3

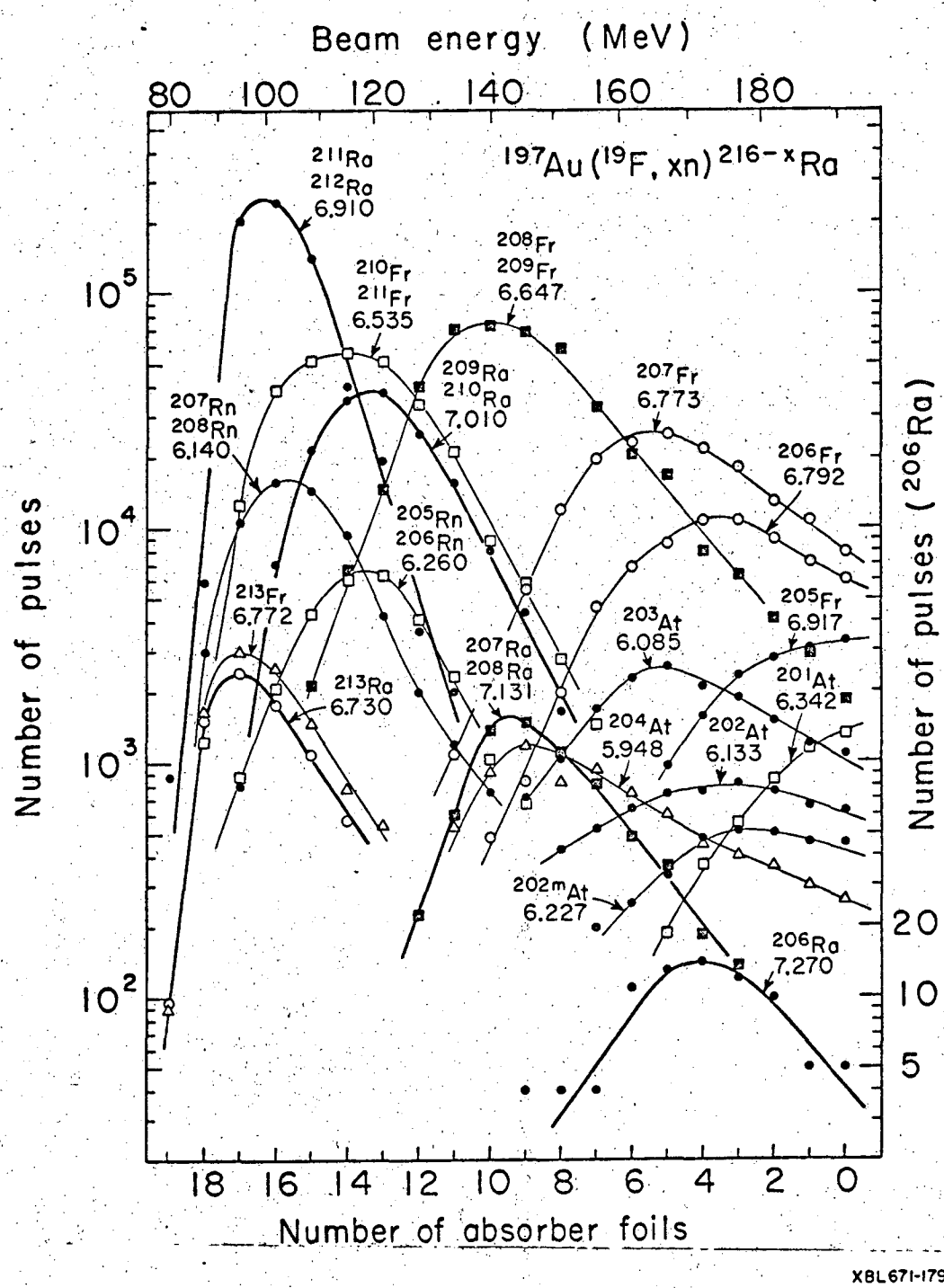
Beam energy (MeV)
80 100 120 140 160 180
$^{197}Au(^{19}F, xn)^{216-x}Ra$
^{211}Ra
^{212}Ra
6.910
^{210}Fr
^{211}Fr
6.535
^{208}Fr
^{209}Fr
6.647
^{209}Ra
^{210}Ra
7.010
^{207}Fr
6.773
^{206}Fr
6.792
^{207}Rn
^{208}Rn
6.140
^{205}Rn
^{206}Rn
6.260
^{213}Fr
6.772
^{205}Fr
6.917
^{203}At
6.085
^{207}Ra
^{208}Ra
7.131
^{213}Ra
6.730
^{201}At
6.342
^{204}At
5.948
^{202}At
6.133
^{202m}At
6.227
^{206}Ra
7.270
Number of pulses
10^5
10^4
10^3
10^2
Number of pulses (^{206}Ra)
20
10
5
18 16 14 12 10 8 6 4 2 0
Number of absorber foils
XBL671-179A

Fig. 4

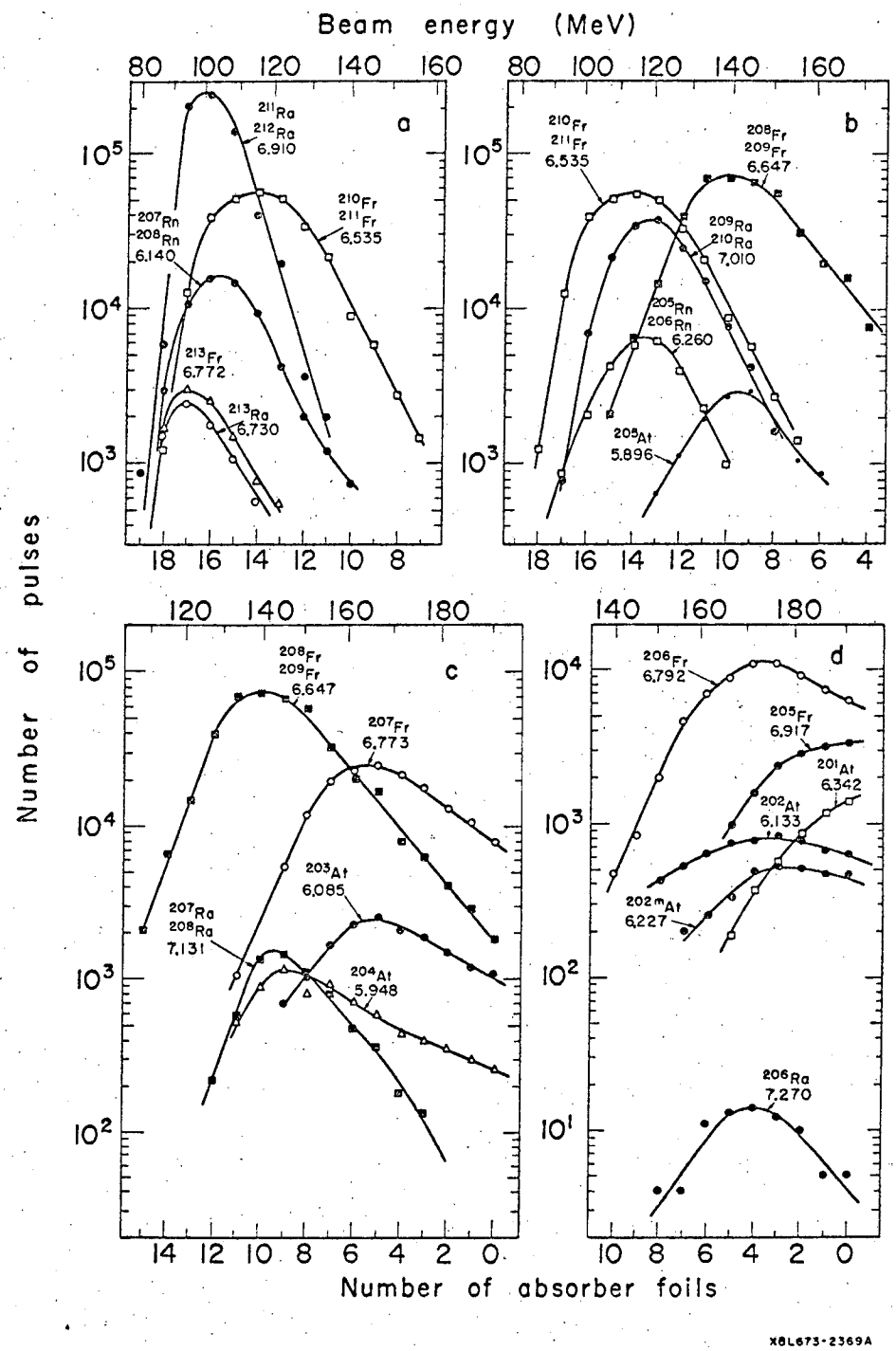
Beam energy (MeV)
Number of pulses
Number of absorber foils
a
b
c
d
211Ra
212Ra
6.910
210Fr
211Fr
6.535
207Rn
208Rn
6.140
213Fr
6.772
213Ra
6.730
208Fr
209Fr
6.647
209Ra
210Ra
7.010
205Rn
206Rn
6.260
205At
5.896
207Fr
6.773
203At
6.085
207Ra
208Ra
7.131
204At
5.948
206Fr
6.792
205Fr
6.917
201At
6.342
202At
6.133
202mAt
6.227
206Ra
7.270
X8L673-2369A

Fig. 5

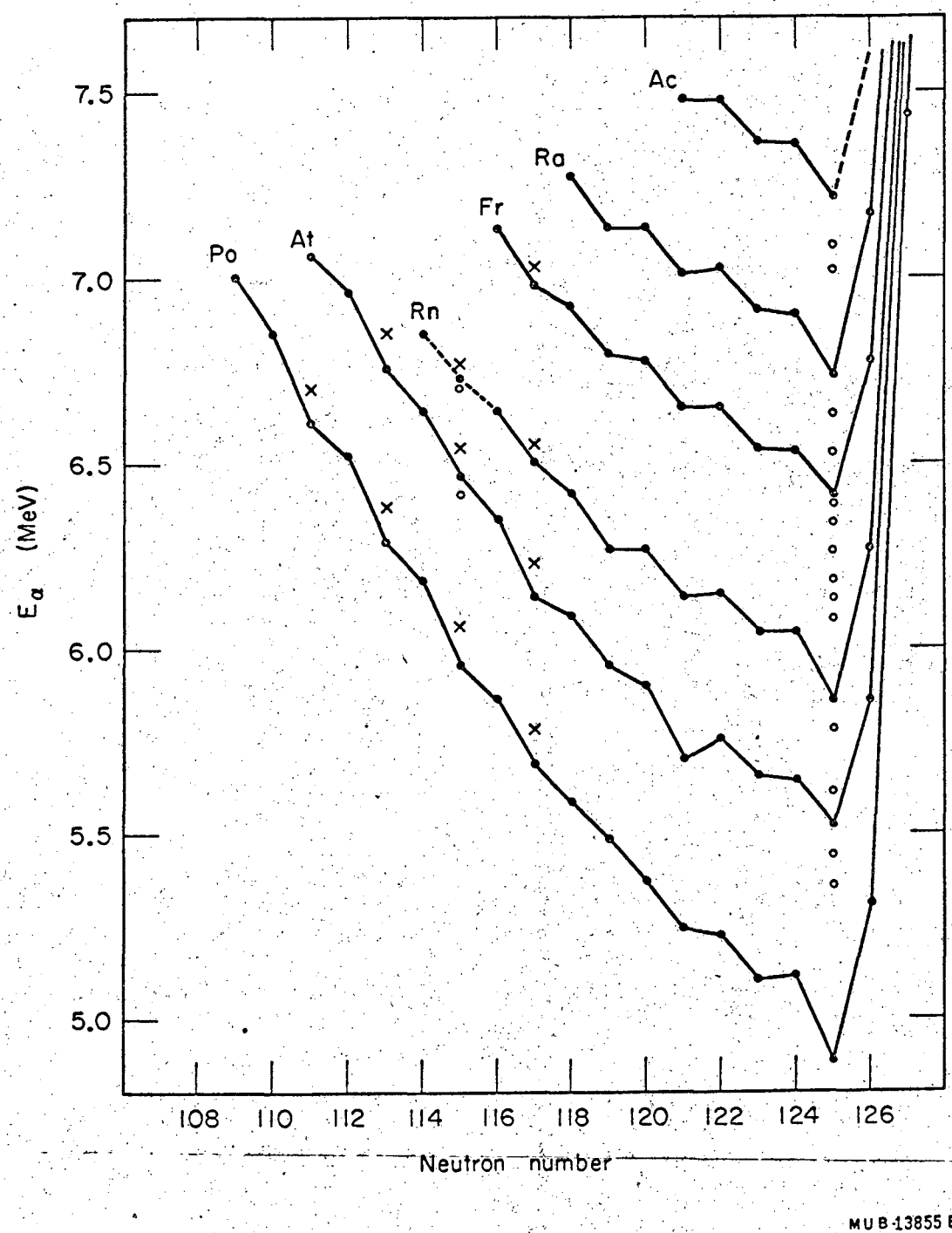
Ac
Ra
Fr
Rn
At
Po
7.5
7.0
6.5
6.0
5.5
5.0
E_α (MeV)
108
110
112
114
116
118
120
122
124
126
Neutron number
MUB-13855 B

Fig. 6

This report was prepared as an account of Government sponsored work. Neither the United States, nor the Commission, nor any person acting on behalf of the Commission:

A. Makes any warranty or representation, expressed or implied, with respect to the accuracy, completeness, or usefulness of the information contained in this report, or that the use of any information, apparatus, method, or process disclosed in this report may not infringe privately owned rights; or

B. Assumes any liabilities with respect to the use of, or for damages resulting from the use of any information, apparatus, method, or process disclosed in this report.

As used in the above, "person acting on behalf of the Commission" includes any employee or contractor of the Commission, or employee of such contractor, to the extent that such employee or contractor of the Commission, or employee of such contractor prepares, disseminates, or provides access to, any information pursuant to his employment or contract with the Commission, or his employment with such contractor.